VOLUME 31 · NUMBER 13 · MAY 1 2013

JOURNAL OF CLINICAL ONCOLOGY

BIOLOGY OF NEOPLASIA

New Syndrome of Paraganglioma and Somatostatinoma Associated With Polycythemia

Karel Pacak, Ivana Jochmanova, Tamara Prodanov, Chunzhang Yang, Maria J. Merino, Tito Fojo, Josef T. Prchal, Arthur S. Tischler, Ronald M. Lechan, and Zhengping Zhuang

Karel Pacak, Ivana Jochmanova, and Tamara Prodanov, Eunice Kennedy Shriver National Institute of Child Health and Human Development; Maria J. Merino and Tito Fojo, National Cancer Institute; Chunzhang Yang and Zhengping Zhuang, National Institute of Neurological Disorders and Stroke, National Institutes of Health, Bethesda, MD; Josef T. Prchal, University of Utah School of Medicine and VA Hospital, Salt Lake City, UT; and Arthur S. Tischler and Ronald M. Lechan, Tufts Medical Center, Boston, MA.

Published online ahead of print at www.jco.org on March 18, 2013.

Supported by the Intramural Research Program of the National Institutes of Health, Eunice Kennedy Shriver National Institute of Child Health and Human Development, and National Institute of Neurological Disorders and Stroke.

I.J., T.P., and C.Y. contributed equally to this work.

Authors' disclosures of potential conflicts of interest and author contributions are found at the end of this article.

Corresponding author: Karel Pacak, MD, PhD, DSc, Section on Medical Neuroendocrinology, Program in Reproductive and Adult Endocrinology, Eunice Kennedy Shriver NICHD, NIH, Building 10, CRC, Room 1E-3140, 10 Center Dr, MSC-1109, Bethesda, MD 20892-1109; e-mail: karel@mail.nih.gov.

0732-183X/13/3113w-1690w/$20.00

DOI: 10.1200/JCO.2012.47.1912

ABSTRACT

Purpose
The occurrence of ≥ two distinct types of tumors, one of them paraganglioma (PGL), is unusual in an individual patient, except in hereditary cancer syndromes.

Patients and Methods
Four unrelated patients were investigated, with thorough clinical evaluation. Plasma and tissue catecholamines and metanephrines were measured by high-performance liquid chromatography. Anatomic and functional imaging were performed for tumor visualization. Germline and tumor tissue DNA were analyzed for hypoxia-inducible factor 2 alpha (*HIF2A*) mutations. The prolyl hydroxylation and stability of the mutant HIF2α protein, transcriptional activity of mutant *HIF2A*, and expression of hypoxia-related genes were also investigated. Immunohistochemical staining for HIF1/2α was performed on formalin-fixed, paraffin-embedded tumor tissue.

Results
Patients were found to have polycythemia, multiple PGLs, and duodenal somatostatinomas by imaging or biochemistry with somatic gain-of-function *HIF2A* mutations. Each patient carried an identical unique mutation in both types of tumors but not in germline DNA. The *HIF2A* mutations in these patients were clustered adjacent to an oxygen-sensing proline residue, affecting HIF2α interaction with the prolyl hydroxylase domain 2–containing protein, decreasing the hydroxylation of HIF2α, and reducing HIF2α affinity for the von Hippel–Lindau protein and its degradation. An increase in the half-life of HIF2α was associated with upregulation of the hypoxia-related genes *EPO*, *VEGFA*, *GLUT1*, and *END1* in tumors.

Conclusion
Our findings indicate the existence of a new syndrome with multiple PGLs and somatostatinomas associated with polycythemia. This new syndrome results from somatic gain-of-function *HIF2A* mutations, which cause an upregulation of hypoxia-related genes, including *EPO* and genes important in cancer biology.

J Clin Oncol 31:1690-1698. © 2013 by American Society of Clinical Oncology

INTRODUCTION

Paraganglioma (PGL) and somatostatinoma are tumors arising from distinct types of neuroendocrine cells. PGLs arise from chromaffin or chromaffin-like cells that develop during embryogenesis from neural crest cells.[1] As these neuroendocrine cells migrate, they populate the adrenal medulla and extra-adrenal paraganglia associated with paraxial sympathetic nerve fibers and branches of the vagus and glossopharyngeal nerves in the head and neck, including the carotid body.[1] In contrast, somatostatinomas develop from enteric endocrine cells currently believed to arise from the endoderm.[2] Despite their different origins, neuroendocrine cells of the paraganglia and GI tract share the ability to secrete specific peptides or amines, as do C cells of the thyroid and neuroendocrine cells found in the lungs, pituitary gland, brain, and other tissues.[1,3] Neuroendocrine tumors (NETs) are distinguished by their location, the cell or tissue type from which they arise, and their specific hormonal secretion.

The occurrence of ≥ two distinct types of NETs in an individual patient is unusual, except in patients with hereditary syndromes such as von Hippel–Lindau (VHL) disease, neurofibromatosis 1 (NF1), mutations in the succinate dehydrogenase (*SDH*) subunits, and multiple endocrine neoplasia (MEN) types 1 and 2.[4,5] In this study, we investigated the clinical and genetic characteristics of four female patients who presented to the National Institutes of

Health (NIH) and Tufts Medical Center with PGL, somatostatinoma, and polycythemia.

PATIENTS AND METHODS

Laboratory Analyses

Mutation analysis, hydroxylation assays, real-time polymerase chain reaction (PCR), and chromatin immunoprecipitation were performed as previously described.[6]

High-Performance Liquid Chromatography

Plasma and tissue catecholamines and metanephrines were measured by liquid chromatography with electrochemical detection.[7]

Immunohistochemistry

Immunohistochemical staining was performed on formalin-fixed, paraffin-embedded tissue. After deparaffinization and heat-induced antigen retrieval using 1 mmol/L ethylenediaminetetraacetic acid, we used a commercially available somatostatin rabbit polyclonal antibody (Cell Marque; DAKO, Carpinteria, CA) for the diagnosis of somatostatinoma, a rabbit polyclonal antibody for hypoxia-inducible factor 1 alpha (HIF1α; Sigma-Aldrich, St Louis, MO), and a mouse monoclonal antibody for HIF2α (Abcam, Cambridge, MA). Primary antibodies were detected using a peroxidase-labeled polymer conjugated to immunoglobulins (DAKO) with 3,3′-diaminobenzidine as a chromogen.

Quantitative Real-Time PCR

Total RNA was extracted from microdissected tumor specimens and normal adrenomedullary tissue. mRNA was reverse transcribed to cDNA and examined by real-time PCR on the Eco Real-Time PCR System (Illumina, San Diego, CA). Erythropoietin (*EPO*) (HP200740; OriGene, Rockville, MD) and *GAPDH* (QT01192646; Qiagen, Hilden, Germany) primer sets were used.

Patient Evaluation

Patients were evaluated under a protocol approved by the *Eunice Kennedy Shriver* National Institute of Child Health and Human Development Institutional Review Board. All patients provided written informed consent. Anatomic imaging; positron emission tomography (PET) studies using ^{18}F-fluorodopamine, ^{18}F-fluorodopa, and [^{18}F]fluorodeoxyglucose ([^{18}F]FDG); and ^{123}I-metaiodobenzylguanidine (^{123}I-MIBG) scintigraphy were performed.[8] In two patients, computed tomography (CT) scans with negative contrast were used to better detect duodenal tumors.

Case Series

Patient 1. A 31-year-old white woman from Serbia had presented with polycythemia since birth (Table 1), managed with phlebotomies. At age 14 years, she was found to have a tumor in the left para-aortic region and hepatosplenomegaly. The patient started to experience headaches, diaphoresis, night sweats, fatigue, heat intolerance, nausea and vomiting, and blurred vision. At age 23 years, she presented with blood pressure of 180/100 mmHg. Abdominal magnetic resonance imaging revealed multiple tumors. The patient underwent surgical resection, with histopathology consistent with PGLs. After resection, her hemoglobin (HgB), hematocrit (Hct), and EPO levels decreased (Table 1). One year later, follow-up abdominal CT imaging showed a 1-cm lesion around the left renal vein and another close to the inferior vena cava, with both enlarging during the next year. Blood tests revealed elevated Hgb, chromogranin A, and norepinephrine (NE) levels. An echocardiogram showed an ascending aorta aneurysm. Two years later, whole-body magnetic resonance imaging and ^{123}I-MIBG scintigraphy showed multiple abdominal tumors, hepatosplenomegaly, aneurysm of the ascending aorta, pericardial cyst, and mitral valve prolapse. Laboratory evidence indicated recurrence of polycythemia (Table 1). At age 29 years, the patient was referred to NIH (admission findings listed in Table 1).

Imaging studies confirmed multiple abdominal masses and also showed multiple duodenal lesions. The patient underwent surgery. Histopathology confirmed duodenal somatostatinomas, multiple extra-adrenal PGLs, and cholecystitis (Table 1). After surgery, her Hct and Hgb levels normalized, most likely as a result of blood loss during surgery, but her serum EPO levels remained high, most likely resulting from remaining tumors, which were detected on follow-up imaging 1 year later (Table 1).

Patient 2. A 46-year-old white woman of Irish origin had presented from birth with pink cheeks. At age 7 years, she was diagnosed with polycythemia. Her only available blood test results at ages 15 and 19 years are listed in Table 1. From ages 26 to 27 years, the patient reported transient episodes of palpitations, nausea, headache, and anxiety. At age 35 years, she presented to the hospital with dark urine and jaundice. An ultrasound showed dilation of the common bile and pancreatic ducts and a 4-cm cystic mass in the retroperitoneum, posterior to the pancreas. A CT scan of the abdomen and pelvis demonstrated the left retroperitoneal mass, lymphadenopathy, biliary and pancreatic ductal dilation, and possible ampullary or duodenal intraluminal masses. She underwent a Whipple resection; histopathology confirmed abdominal extra-adrenal PGL, two duodenal somatostatinomas, and cholecystitis (Table 1). Metanephrine and somatostatin levels were not measured before surgery.

After surgery, her EPO levels were high, with normal Hct, HgB, RBC, WBC, and platelet counts. Plasma (Table) and urine metanephrine levels were elevated postoperatively. ^{123}I-MIBG scintigraphy showed uptake in the left parasagittal midabdomen and two foci in the para-aortic regions of the central upper and lower abdomen, confirmed by CT. At age 36 years, the patient was referred to NIH for evaluation. ^{18}F-fluorodopamine PET/CT revealed a mass in the upper abdomen to the left of the midline, with a smaller focus located medially. Two additional left para-aortic lesions were found in the mid to lower abdomen, with another small focus in or adjacent to the liver. The patient received ^{131}I-MIBG therapy and, 1 year later, underwent resection of a 4.3-cm para-aortic PGL and several para-aortic lymph nodes. Two of eight lymph nodes contained microscopic foci of paraganglionic tissue in the periphery, interpreted as either hyperplastic paraganglionic tissue contiguous with the lymph nodes or metastatic tumors.

Since surgery, she has had only mildly elevated urine normetanephrine (NMN) levels. The most recent abdominal CT showed a stable 1.1-cm para-aortic mass and slightly enlarged retroperitoneal lymph nodes, unchanged over 6 years. ^{18}F-fluorodopamine and ^{18}F-fluorodopa PET/CT showed seven foci of radiotracer uptake (Figs 1A and 1B). Somatostatin levels have remained in the high to normal range since surgery (Table 1). She has not required phlebotomies since her first surgery; in fact, she developed anemia associated with iron and vitamin B_{12} deficiency as a result of the Whipple resection. With vitamin B_{12} and iron replacement, she has maintained normal HgB and Hct levels.

Patient 3. A 22-year-old white woman had presented with polycythemia since birth. The earliest available blood tests are summarized in Table 1. At age 15 years, she experienced episodes of severe headache, tachycardia, shakiness, and shortness of breath. At age 18 years, she developed episodes of shakiness, tachycardia, decreased exercise tolerance, dizziness, and exercise-associated nausea. She was found to have blood pressure of 180/130 mmHg and was referred to NIH for evaluation (admission findings listed in Table 1). A CT scan of the chest, abdomen, and pelvis demonstrated a left renal cystic lesion, partially necrotic right adrenal mass, and mass inferior to the aortic bifurcation. ^{123}I-MIBG scintigraphy showed radiotracer uptake in the right adrenal gland area and another focus around the organ of Zuckerkandl. The patient underwent surgical resection of the tumors, and histopathology confirmed multiple PGLs. EPO and somatostatin levels before surgery were retrospectively measured at NIH in 2012 (Table 1). Follow-up 2 years later revealed para-aortic and aortocaval foci on [^{18}F]FDG PET/CT and high levels of NE, NMN, and EPO (Table 1). Histopathology after surgical resection again confirmed multiple PGLs. After surgery, her EPO level decreased (Table 1). Because of high plasma somatostatin levels, a follow-up CT scan using water in place of conventional enteric contrast material was performed to increase the detection sensitivity for a duodenal mass. This technique revealed a 1-cm mass extending into the lumen of the distal second portion of duodenum, a small mass in the second portion of duodenum, a small paraduodenal/parapancreatic node near the head of pancreas (Figs 1C and 1D), and cholecystolithiasis. The histopathology and immunohistochemistry of the duodenal tumors were

Table 1. Demographics and Laboratory and Imaging Findings of Index Patients

Demographic/Finding	Patient 1								Patient 2				
	Birth	Before Surgery (age 23 years)	After Surgery (age 23 years)	Age 26 Years*	Age 27 Years*	NIH (age 29 years)	After Surgery at NIH (age 29 years)	Recent Follow-Up (age 31 years)*	Age 15 Years†	After First Surgery (age 35 years)	NIH (age 36 years)	Recent Follow-Up at Tufts Medical Center (age 44 years)	Recent Follow-Up at NIH (age 44 years)
Origin	Serbian								Irish				
Sex	Female								Female				
Blood count and EPO‡													
RBC, per L (3.93 to 5.22 × 10^{12})	7.06 × 10^{12}	8.9 × 10^{12}	7.07 × 10^{12}	7.9 × 10^{12}	8.4 × 10^{12}	7.78 × 10^{12}	5.8 × 10^{12}	8.52 × 10^{12}	6.77 × 10^{12}	5.06 × 10^{12}	4.94 × 10^{12}	5.27 × 10^{12}	4.74 × 10^{12}
Hct, % (34.1 to 44.9)	76.0	60.0	48.6	43.0	48.0	50.5	39.5	50.4	60.0 (at age 19 years)	30.5	32.6	37.6	33.0
HgB, g/dL (11.2 to 15.7)	20.1	18.6	13.8	13.0	14.5	14.7	11.3	14.1	15.9	8.9	9.2	10.9	9.3
WBC, per L (3.98 to 10.04 × 10^9)	1.12 × 10^9	7.7 × 10^9	8.3 × 10^9	5.8 × 10^9	6.0 × 10^9	7.19 × 10^9	12.5 × 10^9	9.58 × 10^9	6.2 × 10^9	4.18 × 10^9	3.54 × 10^9	4.1 × 10^9	2.54 × 10^9
Platelets, per L (173 to 369 × 10^9)		234 × 10^9	200 × 10^9	466 × 10^9	410 × 10^9	194 × 10^9	1036 × 10^9	465 × 10^9	227 × 10^9	510 × 10^9	214 × 10^9	184 × 10^9	140 × 10^9
EPO, mIU/mL (3.7 to 31.5)		420.0	60.0			150.0	241.0	173.0		182.2	165.0§		159.0
MNs, catecholamines, CgA, and somatostatin (plasma)‡													
NMN, pg/mL (18 to 112)						4,834		688		4,720	515		81
MN, pg/mL (12 to 61)						121		56			22		22
NE, pg/mL (80 to 498)						10,951		519		1,068	775		283
EPI, pg/mL (4 to 83)						100		8		9	9		10
DA, pg/mL (3 to 46)						28		11			6		6
Methoxytyramine, pg/mL (< 14)								< 10					< 10
CgA, ng/mL (≤ 225)						1,640		149		.5 (6 to 39)‡		3.2 (1.9 to 15)‡‖	116
Somatostatin, pg/mL (10 to 25)						109§				17¶	18§¶	26 (10 to 30)‡¶	7¶
Catecholamines in PGL tissue													
DHPG, pg/mg				1,055							NA		
NE, pg/mg				1,901,736							NA		
DOPA, pg/mg				UDL							NA		
EPI, pg/mg				107,800							NA		
DA, pg/mg				17,019							NA		
DOPAC, pg/mg				UDL							NA		
Functional imaging (PET/CT)													
^{18}F-fluorodopamine						++		ND			++		++
^{18}F-fluorodopa						ND		ND			ND		++
[^{18}F]FDG						+		+			+		ND
Gallbladder disease	Cholecystitis								Cholecystitis				

(continued on following page)

Abbreviations: CgA, chromogranin A; CT, computed tomography; DA, dopamine; DHPG, 3,4-dihydroxyphenylglycol; DOPA, 3,4-dihydroxyphenylalanine; DOPAC, 3,4-dihydroxyphenylacetic acid; EPI, epinephrine; EPO, erythropoietin; FDG, fluorodeoxyglucose; Hct, hematocrit; HgB, hemoglobin; MN, metanephrine; MNs, metanephrines (metanephrine or normetanephrine); NA, not available; ND, not done; NE, norepinephrine; NIH, National Institutes of Health; NMN, normetanephrine; PET, positron emission tomography; PGL, paraganglioma; UDL, under detection limit.

*Results of patient 1 were obtained while she was treated by regular phlebotomies.

†Patient presented with pink cheeks from birth.

‡Ranges indicate normal reference limits of various biochemical tests.

§Values were measured retrospectively at NIH in 2012.

‖ Levels of CgA could be biased because patient receives proton-pump inhibiting medication.

¶Somatostatin levels are after resection of somatostatinoma.

Table 1. Demographics and Laboratory and Imaging Findings of Index Patients (continued)

Demographic/Finding	Patient 3								Patient 4							
	Age 1 Year	Age 14 Years	Age 18 Years	Before Surgery at NIH (age 18 years)	After Surgery at NIH (age 18 years)	Before Second Surgery (age 21 years)	After Second Surgery (age 21 years)	Recent Follow-Up (age 22 years)	Before First Surgery (age 17 years)	January 2004 (age 17 years)	Age 20 Years	Admission to NIH (age 20 years)	Before Surgery at NIH (age 20 years)	After Surgery at NIH (age 20 years)	Follow-Up Outside of NIH (age 21 years)	Recent Follow-Up at NIH (age 25 years)
Origin	American (white)								Chinese							
Sex	Female								Female							
Blood count and EPO‡																
RBC, per L (3.93 to 5.22 × 10^{12})	8.64 × 10^{12}	7.66 × 10^{12}	6.29 × 10^{12}	7.85 × 10^{12}	7.14 × 10^{12}	7.3 × 10^{12}	6.92 × 10^{12}	7.37 × 10^{12}	9.02 × 10^{12}		10.26 × 10^{12}	10.48 × 10^{12}	10.4 × 10^{12}	8.66 × 10^{12}	9.68 × 10^{12}	8.89 × 10^{12}
Hct, % (34.1 to 44.9)	63.2	56.5	62.3	59.3	54.5	55.4	55.3	54.9	49.1		56.9	59.6	59.4	49.8	55.0	47.7
HgB, g/dL (11.2 to 15.7)	20.3	18.5	20	18.8	16.6	17.6	17.0	17.7	14.9		17.2	17.3	17.1	14.8	16.0	14.9
WBC, per L (3.98 to 10.04 × 10^9)	9.9 × 10^9	10.6 × 10^9	15.2 × 10^9	8.13 × 10^9	5.86 × 10^9	13.8 × 10^9	11.17 × 10^9	11.76 × 10^9	8.37 × 10^9		7.2 × 10^9	9.23 × 10^9	8.92 × 10^9	4.55 × 10^9	6.5 × 10^9	8.95 × 10^9
Platelets, per L (173 to 369 × 10^9)	163 × 10^9	292 × 10^9	267 × 10^9	249 × 10^9	226 × 10^9	211 × 10^9	215 × 10^9	188 × 10^9	220 × 10^9		200 × 10^9	164 × 10^9	120 × 10^9	240 × 10^9	190 × 10^9	184 × 10^9
EPO, mIU/mL (3.7 to 31.5)		155.0 (3.8 to 20.5)	86.2	34.8§		230.0	43.6	32.0		154.0		90.2§				136.0
MNs, catecholamines, CgA, and somatostatin (plasma)‡																
NMN, pg/mL (18 to 112)				858		267	28	27				291	324	83		220
MN, pg/mL (12 to 61)				9		23	< 5	< 5				32	50	< 52		14
NE, pg/mL (80 to 498)				1,760	333	506	193	281				738	1,168	207		526
EPI, pg/mL (4 to 83)				7	< 11	9	6	< 5				30	23	24		5
DA, pg/mL (3 to 46)				20	< 12	9	7	5				10		11		9
Methoxytyramine, pg/mL (< 14)								< 10								< 10
CgA, ng/mL (≤ 225)				320	150	155	106	90				105	270			
Somatostatin, pg/mL (10 to 25)				50§				25				40§				12
Catecholamines in PGL tissue																
DHPG, pg/mg				UDL									UDL			
NE, pg/mg				2,586,655									2,409,948			
DOPA, pg/mg				2,185									5,160			
EPI, pg/mg				35,715									37,173			
DA, pg/mg				4,186									11,946			
DOPAC, pg/mg				UDL									UDL			
Functional imaging (PET/CT)																
^{18}F-fluorodopamine				++		ND						++				++
^{18}F-fluorodopa				++		ND						++				++
[^{18}F]FDG				+		+						+				+
Gallbladder disease	Cholecystolithiasis								Cholecystolithiasis							

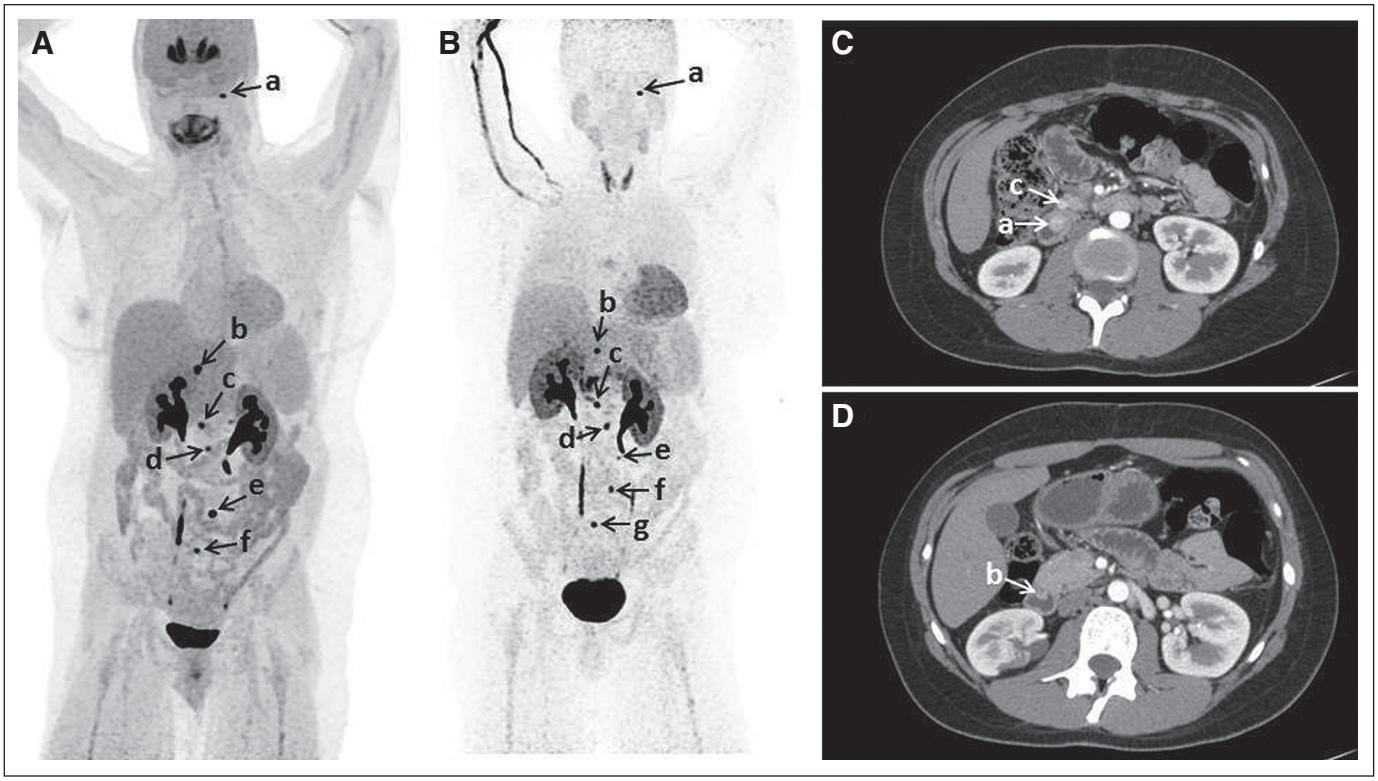

Fig 1. Functional and anatomic imaging. (A) ^{18}F-fluorodopa positron emission tomography (PET)/computed tomography (CT) in patient 2 showing (a) small focus at base of skull consistent with glomus jugulare tumor, (b) focus at medial edge of liver, (c) aortocaval node at L1/L2 vertebral disc level, (d) another aortocaval focus at L2/L3 vertebral disc level, (e) left periaortic focus at L4/L5 disc level, and (f) right presacral focus in upper pelvis. (B) ^{18}F-fluorodopamine PET/CT in patient 2 also showed (a) focus at base of skull, (b) focus at medial edge of liver or in adjacent node, (c) aortocaval node at L1/L2 disc level, (d) another aortocaval focus at L2/L3 vertebral disc level, (e) left periaortic focus at L3/L4 disc level (not seen on ^{18}F-fluorodopa PET/CT), (f) probable common iliac node at L4/5 disc level, and (g) presacral focus on right in upper pelvis. (C, D) Early arterial phase of axial CT of abdomen performed with negative enteric contrast in patient 3 showed (a) mass protruding into lumen in distal second portion of duodenum, near junction with third portion, (b) paraduodenal/parapancreatic node, and (c) another small mass in second portion of duodenum.

consistent with somatostatinoma. The latest laboratory findings did not show increased metanephrines, catecholamines, or EPO level (Table 1).

Patient 4. A 22-year-old woman of Chinese origin presented with ruddy complexion and red lips at age 4 and was diagnosed with polycythemia at age 5 years. At age 15 years, she experienced exercise-associated nausea. At age 17 years, she presented with malignant hypertension (200/140 mmHg). A CT scan revealed two paraspinal masses below the left renal hilum. ^{123}I-MIBG scintigraphy showed four foci in the left paravertebral area. The patient had elevated urine NE (exact value not available); her blood count is shown in Table 1. The patient underwent surgery; histopathology confirmed multiple PGLs. After surgery, urine NE decreased to within normal limits. At age 20 years, the patient underwent a cholecystectomy because of cholecystolithiasis, and elevated urine NMN and NE were noted. The patient started to experience recurrent hypertensive episodes, was found to have elevated urine NE and NMN levels, and was referred to NIH for evaluation (admission findings listed in Table 1). Anatomic and functional imaging revealed two nodules in the left para-aortic area and in the right retroperitoneum at the level of the right kidney and a lesion in the liver, compatible with a hemangioma. The patient underwent surgical resection of the tumors; histopathology confirmed extra-adrenal PGLs. At age 21 years, follow-up [^{18}F]FDG PET/CT revealed a hypermetabolic nodule near the left adrenal gland. The patient underwent another surgery to remove two small PGLs in this region. Since the second surgery, she has required infrequent phlebotomies. On a recent follow-up CT (at age 25 years), two abdominal lesions were found, and possible atypical lesions in the distal duodenum and near the pancreas could not be excluded. The CT study of the duodenum was limited because of subdistended bowel. ^{18}F-fluorodopa PET/CT showed two abnormal areas of uptake in the upper abdomen, a small focus in the right caval region, and another small focus in the upper outer quadrant of the left breast. ^{18}F-fluorodopamine PET/CT confirmed the two small foci in the upper abdomen and revealed two foci in the right caval region. Laboratory findings show persistently elevated NMN, NE, and EPO levels (Table 1).

Tissue Analysis

Genetic testing in all the patients revealed *HIF2A* somatic mutations in the tumors, clustered adjacent to an oxygen-sensing proline residue (Table 2). These mutations reduced HIF2α hydroxylation by prolyl hydroxylase and binding to the VHL protein, resulting in proteins four- to six-fold more stable than wild-type *HIF2A* (Table 2) that could be readily detected in the patients' tumors (Fig 2A). Mimicking hypoxic conditions, expression of genes downstream of *HIF2A*, including *EPO*, *VEGFA*, *GLUT1*, and *EDN1*, was increased in the PGLs and somatostatinomas compared with normal human adrenomedullary tissue (Table 2). EPO mRNA expression was substantially higher in somatostatinomas and PGLs with somatic *HIF2A* mutations than in other PGLs (Fig 2B).

DISCUSSION

The four patients described here developed two distinct NETs—PGL and duodenal somatostatinoma (histologically confirmed in patients 1 to 3)—associated with polycythemia. PGLs are rare catecholamine-producing tumors derived from chromaffin cells of the extra-adrenal paraganglia.[13] Those arising from the adrenal medulla are called pheochromocytomas. Approximately one third of these tumors have thus far been shown to be hereditary, including those associated with *VHL*, *NF1*, *RET* proto-oncogene, and *SDHB*/*C*/*D* subunit mutations and, recently, those associated with mutations in *SDHA*, *SDHAF2*,

Table 2. Somatic Mutations, *HIF2α* Transcriptional Activity, Stability, Binding Efficacy, and *HIF2α* Downstream Gene Expression in Tumor Tissue of Index Patients

Characteristic	Patient 1		Patient 2		Patient 3		Patient 4
	PGL	Somatostatinoma	PGL	Somatostatinoma	PGL	Somatostatinoma	PGL
Somatic mutation in *HIF2A*	c.1588G>A p.A530T		c.1595A>G p.Y532C		c.1589C>T p.A530V		c.1586T>C p.L529P
Protein half-life compared with wild-type protein, minutes (wild type, 14.4)*	57.6		40.1		79.8		40.2
Affinity to VHL protein†	Decreased		Decreased		Decreased		Decreased
Pro531 hydroxylation‡	Decreased		Decreased		Decreased		Decreased
Transcription activity§	Intact binding efficiency to HRE domain in genomic DNA		Intact binding efficiency to HRE domain in genomic DNA		Intact binding efficiency to HRE domain in genomic DNA		Intact binding efficiency to HRE domain in genomic DNA
Somatic mutation in *HIF2A* downstream gene expression in tumor tissue, mRNA‖							
EPO	Increased	Increased	Increased	Increased	Increased		Increased
VEGF	Increased	Increased	Increased	Increased	Increased		Increased
EDN1	Increased	Increased	Increased	Increased	Increased		Increased
GLUT1	Increased	Increased	Increased	Increased	Increased		Increased

Abbreviations: DMT1, divalent metal transporter 1; EDN1, endothelin 1; EPO, erythropoietin; GLUT1, glucose transporter 1; HIF2α, hypoxia-inducible factor 2α; HRE, hypoxia-responsive element; MALDI-TOF, matrix-assisted laser desorption/ionization time-of-flight mass spectrometer; PGL, paraganglioma; VEGF, vascular endothelial growth factor; VHL, von Hippel–Lindau.

*Protein half-life was calculated by cycloheximide assay.[9,10]

†Affinity to VHL protein was measured by immunoprecipitation and peptide binding assay.[6]

‡Pro531 hydroxylation was determined by measuring peptide mass through MALDI-TOF.[11]

§Transcription activity of *HIF2α* was determined by its affinity to HRE in *DMT1* gene promoter via chromatin immunoprecipitation assay.[12]

‖Hypoxia-related gene expression was measured by quantitative polymerase chain reaction.[11]

TMEM127, *MAX*, *PHD2*/*EGLN1*, and *HIF2α*.[4,6] Some of these genes (*VHL* and *SDHB*/*C*/*D*) are involved in HIFα regulation.

Somatostatinomas, rare NETs of the GI tract, were first described in the pancreas and duodenum in 1977.[14] Somatostatinomas account for < 1% of NETs of the GI tract,[15] with an annual incidence of one case per 40 million people.[16] They are occasionally found in patients with VHL or MEN type 1 or 2.[17]

An association of somatostatinoma and PGL has been described rarely in patients with NF1.[18,19] In our patients, a diagnosis of NF1 was ruled out based on clinical grounds, as was a diagnosis of VHL or MEN because of the lack of *VHL* or *RET* mutation. Although somatostatinomas may be asymptomatic, patients can develop a somatostatinoma syndrome characterized by diabetes mellitus, steatorrhea, and cholecystolithiasis, as in patients treated with somatostatin analogs.[20] Interestingly, all four patients presented with gallbladder disease, uncommon in this age group and most likely resulting from chronic somatostatin elevation.

Paraganglia and the enteric endocrine system were postulated to arise from a shared neural crest progenitor.[21] Although this hypothesis seemed to be disproven by subsequent embryologic studies,[2,22] differentiation of both enteroendocrine and neural crest cells is regulated in a similar manner.[23] Moreover, there is a close relationship between the development of neural enteric ganglionic cells and enteroendocrine cells.[24] Thus, at present, although PGL and somatostatinoma seem to have different origins, they share many common features and signaling and developmental pathways. In discussing the embryology of enteroendocrine cells, Fontaine and Le Douarin[22] stated that the possibility of ectodermal cells contributing to the endoderm could not be ruled out, because the endoderm is formed by cells migrating from the upper germ layer through Hensen's node and the primitive streak. This could explain the identical somatic mutations in PGLs and somatostatinomas.

The occurrence of PGL with tumor-induced polycythemia has been reported in only a few patients.[25,26] The first co-occurrence of PGL, duodenal somatostatinoma, and polycythemia was described in a patient with a clinical diagnosis of VHL.[27] In that report, a woman diagnosed with polycythemia at age 9 was found at age 22 years to have multiple PGLs, with increased EPO levels. After tumor removal, the catecholamine, but not the EPO, level normalized. At age 29 years, she was diagnosed with a retinal hemangioblastoma, suggesting VHL type 2A, although genetic testing was not performed. The patient also had a duodenal somatostatinoma.

The patients described in our report did not have a family history of NETs or polycythemia, suggesting either a de novo germline or somatic tumor mutation. The mutations most likely occurred during an early developmental stage, because they seem to be distributed in distinct and distant tumors. Patients 1 and 3 were included in our recent report describing gain-of-function (secondary to a gain in stability) *HIF2α* tumor mutations as a novel mechanism linking PGL and polycythemia, with or without somatostatinomas.[6] Subsequently, the other two patients' tumors were identified to have *HIF2α* mutations. In patient 3, multiple PGLs and multiple somatostatinomas were found; in patient 4, multiple PGLs and elevated plasma somatostatin levels were found, but histopathologic confirmation of somatostatinoma was not performed, because the patient refused an upper GI endoscopy. Recently, the somatostatin level in patient 4 normalized, possibly as a result of treatment with a nonselective combined α- and β-adrenergic antagonist (ie, labetalol), which has been shown to inhibit the release of somatostatin and other neurohormones.[28,29] Furthermore, in some patients, especially those with duodenal somatostatinomas, somatostatin levels may fluctuate, becoming normal or only marginally elevated.[30] In this patient, release of somatostatin from PGLs was ruled out by tumor immunostaining. The normalization of metanephrine and catecholamine levels in patient 2 most

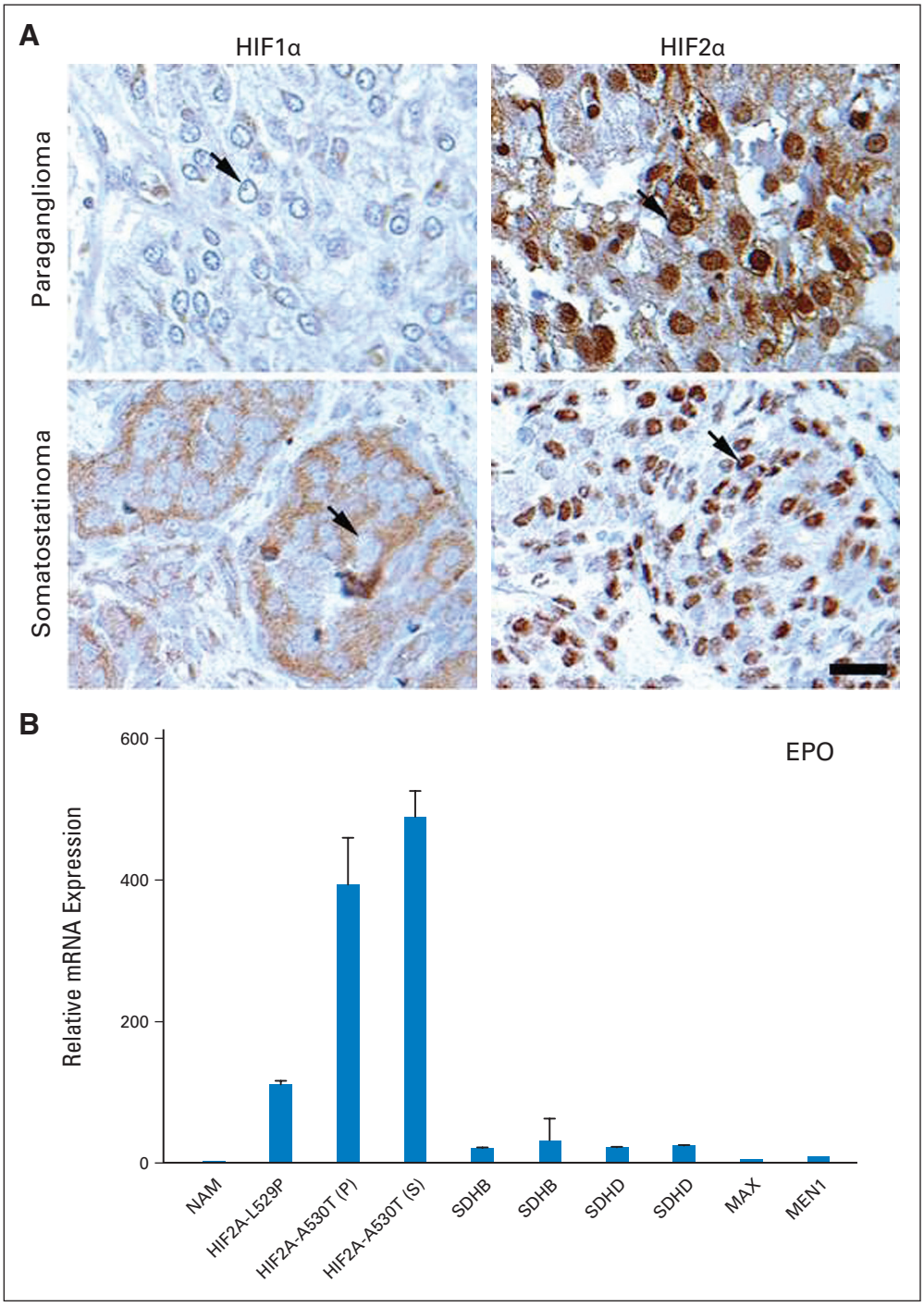

Fig 2. Tumor tissue immunostaining for hypoxia-inducible factor 2 alpha (HIF2α) expression and *EPO* mRNA expression in tumor tissue obtained from patients. (A) Immunohistochemical staining for HIFs in tumor sections (top row, paraganglioma [PGL]; bottom row, somatostinoma) obtained from patient 1, showing nuclear staining (black arrows) for HIF2α (right column) in contrast to HIF1α (left column; scale, 100 mm; magnification, 80×). (B) Comparison of *EPO* mRNA expression assessed by quantitative polymerase chain reaction in PGLs (indicated by P) obtained from patients 1 and 4 and in somatostatinoma obtained from patient 1 (indicated by S) with expression in PGLs from patients with germline *SDHB, SDHD, MAX,* and *RET* mutations, patients with multiple endocrine neoplasia type 1 (MEN1), and patients with normal adrenal medulla (NAM). Bars indicate SE.

probably reflects her reduced tumor burden after the second surgery and ^{131}I-MIBG treatment.[31]

All of the gain-of-function *HIF2α* mutations described in our patients resulted in HIF2α stabilization, by affecting the hydroxylation of proline 531 and in turn the binding of VHL (Table 2). Prolyl hydroxylation of HIFα is a crucial step for its recognition by the VHL protein and its subsequent proteasomal degradation.[32] Thus, disruption of prolyl hydroxylation results in reduced HIF2α degradation but intact transcriptional activity, leading to the activation of downstream hypoxia-related genes. HIF2α is a physiologic regulator of *EPO* transcription; its overexpression is associated with increased EPO production.[33] The clinical presentations of these patients are consistent with dysregulation of HIF2α signaling. First, the PGLs were found to have a typical noradrenergic biochemical phenotype, reflecting the involvement of HIF2α in NE biosynthesis in sympathoadrenal cells.[34,35] Second, the presence of increased tumor mRNA for *EPO*, *GLUT1*, *EDN1*, and *VEGFA* and strong positive immunohistochemical staining, indicative of high HIF2α expression in the tumors (Fig 2), suggest that the clinical phenotypes, including increased erythropoiesis (development of polycythemia), glucose uptake (positive [^{18}F]FDG PET), and

increased angiogenesis, may derive from a common denominator of HIF2α upregulation.

HIF2α is considered the key regulator of erythropoiesis. This association has recently been demonstrated in four patients with activating germline *HIF2A* mutations who developed polycythemia at a young age.[36] Although none of these patients had NETs or other malignancies, hypoxia-dependent or -independent HIF stabilization occurs in many tumors and is proposed to promote proliferation, survival, invasion, and metastasis.[33,37,38] HIF2α stabilization as a result of *PHD2* and *VHL* mutations has also been associated with PGL-related EPO production.[39,40] However, none of our patients were found to have somatic *PHD2* mutations in their tumors.

Figure 3 summarizes the current view of the pathogenesis of various inherited PGLs, which all result in HIF2α stabilization with or without concurrent polycythemia and somatostatinoma. In contrast to all other currently known hereditary PGLs, however, this new syndrome is caused by somatic gain-of-function *HIF2A* mutations. In our patients, the association between HIF2α and EPO production is supported by the decreased EPO levels after removal of the PGLs, except in patient 2, whose EPO level may have remained elevated because of chronic anemia after her Whipple resection, although other sources and mechanisms of EPO production may also have been involved.[43] It would be of interest to investigate whether other tumors, particularly other neuroendocrine tumors, including gastroenteropancreatic ones, have somatic gain-of-function *HIF2A* mutations. Further study is needed to elucidate how this mutation precisely contributes to tumorigenesis and to determine whether some patients with polycythemia should be screened for the presence of NETs or, conversely, whether patients with multiple seemingly sporadic PGLs with or without polycythemia should be screened for the presence of somatostatinomas. Whether this syndrome exists only in women is also unclear at the present time.

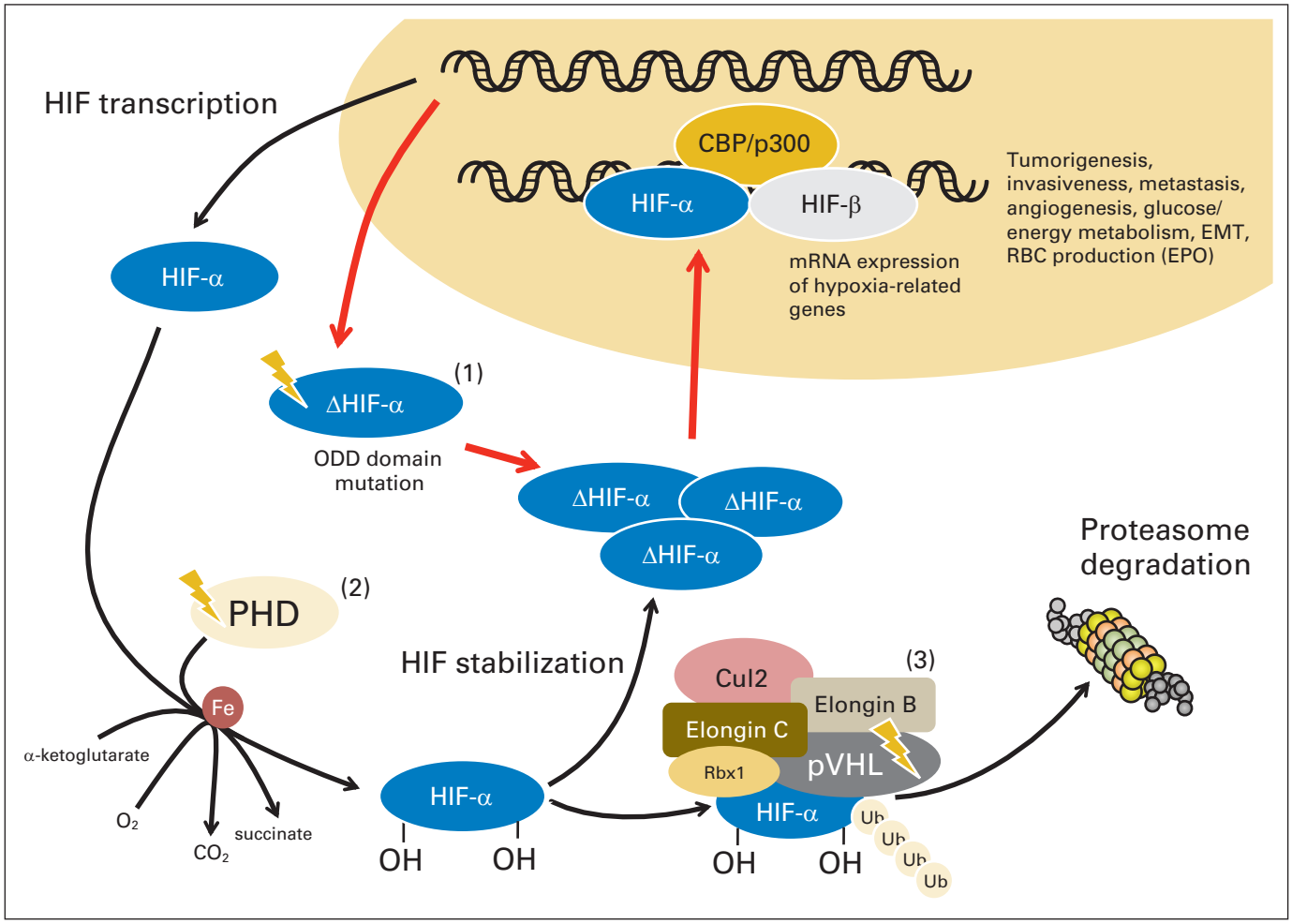

Fig 3. Summary of pathways affecting hypoxia-inducible factor (HIF) turnover involved in development of various paragangliomas (PGLs), some associated with either somatostatinoma or polycythemia. (1) Somatic gain-of-function *HIF2A* mutations have been described in this report to be associated with multiple PGLs, somatostatinoma, and polycythemia. These mutations affect prolyl hydroxylation and pVHL (Von Hippel–Lindau protein) protein binding and reduce HIF2α degradation but not transcriptional activity.[6] pVHL is part of an E3 ubiquitin ligase complex that targets HIFα for proteasomal degradation.[41] Interaction of pVHL with HIFα is determined by hydroxylation status of HIFα proline residues. This hydroxylation is oxygen (O_2) dependent and catalyzed by family of prolyl hydroxylases (PHD1-3). HIFα stabilization can occur as a result of mutations in either *PHD* or *VHL*. (2) Germline mutations in *PHD2* have been associated with congenital polycythemia and extra-adrenal PGLs.[30] (3) *VHL* mutations prevent pVHL from binding hydroxylated HIFα and targeting it for proteasomal degradation. As a result of either *PHD* or *VHL* mutation, HIFα accumulates in cytoplasm, translocates to nucleus, forms heterodimers with HIFβ, and activates transcription of target genes. In pVHL-defective PGLs, there is evidence of increased HIF activity.[42] CBP, cAMP-response element-binding protein; CO_2, carbon dioxide; cul2, cullin 2; EMT, epithelial-mesenchymal transition; EPO, erythropoietin; ODD, oxygen-dependent degradation; OH, hydroxyl group; p300, histone acetyltransferase p300; Rbx1, ring-box 1 protein; Ub, ubiquitin.

AUTHORS' DISCLOSURES OF POTENTIAL CONFLICTS OF INTEREST

The author(s) indicated no potential conflicts of interest.

AUTHOR CONTRIBUTIONS

Conception and design: Karel Pacak, Ivana Jochmanova, Chunzhang Yang, Zhengping Zhuang
Financial support: Karel Pacak
Administrative support: Karel Pacak
Provision of study materials or patients: Karel Pacak, Tamara Prodanov, Maria J. Merino, Josef T. Prchal, Arthur S. Tischler, Ronald M. Lechan, Zhengping Zhuang
Collection and assembly of data: Karel Pacak, Ivana Jochmanova, Tamara Prodanov, Josef T. Prchal, Arthur S. Tischler, Ronald M. Lechan
Data analysis and interpretation: Karel Pacak, Ivana Jochmanova, Tamara Prodanov, Chunzhang Yang, Maria J. Merino, Tito Fojo, Arthur S. Tischler, Ronald M. Lechan, Zhengping Zhuang
Manuscript writing: All authors
Final approval of manuscript: All authors

REFERENCES

1. Adams MS, Bronner-Fraser M: The role of neural crest cells in the endocrine system. Endocr Pathol 20:92-100, 2009
2. Andrew A, Kramer B, Rawdon BB: The origin of gut and pancreatic neuroendocrine (APUD) cells: The last word? J Pathol 186:117-118, 1998
3. Erickson CA, Reedy MV: Neural crest development: The interplay between morphogenesis and cell differentiation. Curr Top Dev Biol 40:177-209, 1998
4. Gimenez-Roqueplo AP, Dahia PL, Robledo M: An update on the genetics of paraganglioma, pheochromocytoma, and associated hereditary syndromes. Horm Metab Res 44:328-333, 2012
5. Lenders JW, Eisenhofer G, Mannelli M, et al: Phaeochromocytoma. Lancet 366:665-675, 2005
6. Zhuang Z, Yang C, Lorenzo F, et al: Somatic HIF2A gain-of-function mutations in paraganglioma with polycythemia. N Engl J Med 367:922-930, 2012
7. Eisenhofer G: Analytical differences between the determination of plasma catecholamines by liquid chromatography with electrochemical detection and by radioenzymatic assay. J Chromatogr 377:328-333, 1986
8. Timmers HJ, Chen CC, Carrasquillo JA, et al: Comparison of 18F-fluoro-L-DOPA, 18F-fluorodeoxyglucose, and 18F-fluorodopamine PET and 123I-MIBG scintigraphy in the localization of pheochromocytoma and paraganglioma. J Clin Endocrinol Metab 94:4757-4767, 2009
9. Yang C, Asthagiri AR, Iyer RR, et al: Missense mutations in the NF2 gene result in the quantitative loss of merlin protein and minimally affect protein intrinsic function. Proc Natl Acad Sci U S A 108: 4980-4985, 2011
10. Lorenzo FR, Yang C, Ng Tang Fui M, et al: A novel EPAS1/HIF2A germline mutation in a congenital polycythemia with paraganglioma. J Mol Med (Berl) [epub ahead of print on October 23, 2012]
11. Percy MJ, Furlow PW, Lucas GS, et al: A gain-of-function mutation in the HIF2A gene in familial erythrocytosis. N Engl J Med 358:162-168, 2008
12. Mastrogiannaki M, Matak P, Keith B, et al: HIF-2alpha, but not HIF-1alpha, promotes iron absorption in mice. J Clin Invest 119:1159-1166, 2009
13. DeLellis RA, Lloyd RV, Heitz PU, et al (eds): Tumours of Endocrine Organs. Lyon, France, IARC Press, 2004
14. Ganda OP, Weir GC, Soeldner JS, et al: "Somatostatinoma": A somatostatin-containing tumor of the endocrine pancreas. N Engl J Med 296:963-967, 1977
15. Delcore R, Friesen SR: Gastrointestinal neuroendocrine tumors. J Am Coll Surg 178:187-211, 1994
16. Taheri S, Ghatei MA, Bloom SR: Gastrointestinal hormones and tumor syndromes, in DeGroot LJ, Jameson, J Larry, et al (eds): Endocrinology (ed 5). Philadelphia, PA, Elsevier Saunders, 2006, pp 3551-3507
17. Vinik AI, Strodel WE, Eckhauser FE, et al: Somatostatinomas, PPomas, neurotensinomas Semin Oncol 14:263-281, 1987
18. Cantor AM, Rigby CC, Beck PR, et al: Neurofibromatosis, phaeochromocytoma, and somatostatinoma. BMJ (Clin Res Ed) 285:1618-1619, 1982
19. Stephens M, Williams GT, Jasani B, et al: Synchronous duodenal neuroendocrine tumours in von Recklinghausen's disease: A case report of co-existing gangliocytic paraganglioma and somatostatin-rich glandular carcinoid. Histopathology 11:1331-1340, 1987
20. Norlén O, Hessman O, Stålberg P, et al: Prophylactic cholecystectomy in midgut carcinoid patients. World J Surg 34:1361-1367, 2010
21. Pearse AG: The cytochemistry and ultrastructure of polypeptide hormone-producing cells of the APUD series and the embryologic, physiologic and pathologic implications of the concept. J Histochem Cytochem 17:303-313, 1969
22. Fontaine J, Le Douarin NM: Analysis of endoderm formation in the avian blastoderm by the use of quail-chick chimaeras: The problem of the neurectodermal origin of the cells of the APUD series. J Embryol Exp Morphol 41:209-222, 1977
23. Takashima S, Adams KL, Ortiz PA, et al: Development of the Drosophila entero-endocrine lineage and its specification by the Notch signaling pathway. Dev Biol 353:161-172, 2011
24. Nakagawa Y, Perentes E: Are intestinal endocrine cells affected in Hirschsprung's disease? An immunohistochemical study with anti-Leu 7 monoclonal antibody. J Pediatr Surg 23:957-961, 1988
25. Dionne JM, Wu JK, Heran M, et al: Malignant hypertension, polycythemia, and paragangliomas. J Pediatr 148:540-545, 2006
26. Imai T, Funahashi H, Sato Y, et al: Multiple functioning paraganglioma associated with polycythemia. J Surg Oncol 39:279-282, 1988
27. Karasawa Y, Sakaguchi M, Minami S, et al: Duodenal somatostatinoma and erythrocytosis in a patient with von Hippel-Lindau disease type 2A. Intern Med 40:38-43, 2001
28. Samols E, Weir GC: Adrenergic modulation of pancreatic A, B, and D cells alpha-adrenergic suppression and beta-adrenergic stimulation of somatostatin secretion, alpha-adrenergic stimulation of glucagon secretion in the perfused dog pancreas J Clin Invest 63:230-238, 1979
29. Richardson SB, Twente S: Inhibition of hypothalamic somatostatin release by beta-adrenergic antagonists. Endocrinology 126:1043-1046, 1990
30. Vinik AI, Silva MP, Woltering EA, et al: Biochemical testing for neuroendocrine tumors. Pancreas 38:876-889, 2009
31. Loh KC, Fitzgerald PA, Matthay KK, et al: The treatment of malignant pheochromocytoma with iodine-131 metaiodobenzylguanidine (131I-MIBG): A comprehensive review of 116 reported patients. J Endocrinol Invest 20:648-658, 1997
32. Kaelin WG Jr: The von Hippel-Lindau tumour suppressor protein: O2 sensing and cancer. Nat Rev Cancer 8:865-873, 2008
33. Patel SA, Simon MC: Biology of hypoxia-inducible factor-2alpha in development and disease. Cell Death Differ 15:628-634, 2008
34. Tian H, Hammer RE, Matsumoto AM, et al: The hypoxia-responsive transcription factor EPAS1 is essential for catecholamine homeostasis and protection against heart failure during embryonic development. Genes Dev 12:3320-3324, 1998
35. Nilsson H, Jögi A, Beckman S, et al: HIF-2alpha expression in human fetal paraganglia and neuroblastoma: Relation to sympathetic differentiation, glucose deficiency, and hypoxia. Exp Cell Res 303:447-456, 2005
36. Percy MJ, Beer PA, Campbell G, et al: Novel exon 12 mutations in the HIF2A gene associated with erythrocytosis. Blood 111:5400-5402, 2008
37. Keith B, Johnson RS, Simon MC: HIF1alpha and HIF2alpha: Sibling rivalry in hypoxic tumour growth and progression. Nat Rev Cancer 12:9-22, 2012
38. Semenza GL: Hypoxia-inducible factors: Mediators of cancer progression and targets for cancer therapy. Trends Pharmacol Sci 33:207-214, 2012
39. Ladroue C, Carcenac R, Leporrier M, et al: PHD2 mutation and congenital erythrocytosis with paraganglioma. N Engl J Med 359:2685-2692, 2008
40. Capodimonti S, Teofili L, Martini M, et al: Von Hippel–Lindau disease and erythrocytosis. J Clin Oncol 30:e137-e139, 2012
41. Kaelin WG Jr: Molecular basis of the VHL hereditary cancer syndrome. Nat Rev Cancer 2:673-682, 2002
42. Dahia PL, Ross KN, Wright ME, et al: A HIF1alpha regulatory loop links hypoxia and mitochondrial signals in pheochromocytomas. PLoS Genet 1:72-80, 2005
43. Lee FS: Genetic causes of erythrocytosis and the oxygen-sensing pathway. Blood Rev 22:321-332, 2008

Acknowledgment

We thank Constantine A. Stratakis, MD, D(med)Sci, and Vera Popovic, MD, PhD, for referring patient 1 and collecting her materials and data; Peter Darwin, MD, and Steve Wank, MD, for evaluating patient 3; Alexander Ling, MD, and Clara C. Chen, MD, for reviewing the imaging studies; Electron Kebebew, MD, for performing the surgeries at the National Institutes of Health; and Karen T. Adams, MS, CRNP, Victoria Martucci, BA, Joey Matro, MD, and Thanh-Truc Huynh, BS, for technical help and assistance with the patients.